

Long-time stable SAV-BDF2 numerical schemes for the forced Navier-Stokes equations

Daozhi Han^a, Xiaoming Wang^b

^a*Department of Mathematics, State University of New York at Buffalo, Buffalo, NY 14260*

^b*School of Mathematical Science, Eastern Institute of Technology, Ningbo, Zhejiang 315200, China*

Abstract

We propose a novel second-order accurate, long-time unconditionally stable time-marching scheme for the forced Navier-Stokes equations. A new Forced Scalar Auxiliary Variable approach (FSAV) is introduced to preserve the underlying dissipative structure of the forced system that yields a uniform-in-time estimate of the numerical solution. In addition, the numerical scheme is autonomous if the underlying model is, laying the foundation for studying long-time dynamics of the numerical solution via dynamical system approach. As an example we apply the new algorithm to the two-dimensional incompressible Navier-Stokes equations. In the case with no-penetration and free-slip boundary condition on a simply connected domain, we are also able to derive a uniform-in-time estimate of the vorticity in H^1 norm in addition to the L^2 norm guaranteed by the general framework. Numerical results demonstrate superior performance of the new algorithm in terms of accuracy, efficiency, stability and robustness.

Keywords: forced autonomous dynamical systems, Navier-Stokes equations, SAV, BDF2, long-time stability

2010 MSC: 35K61, 76T99, 76S05, 76D07.

1. Introduction

Consider the incompressible Navier-Stokes equations (NSE):

$$\frac{\partial \mathbf{u}}{\partial t} + \mathbf{u} \cdot \nabla \mathbf{u} - \frac{1}{Re} \Delta \mathbf{u} = -\nabla p + \mathbf{F}, \quad \nabla \cdot \mathbf{u} = 0, \quad (1.1)$$

equipped with either the no-slip, no-penetration boundary condition, or the no-penetration plus free slip boundary condition, or the periodic boundary condition. Throughout it is assumed that the L^2 norm of the body force \mathbf{F} is uniformly bounded in time. Under these assumptions it is known that in 2D \mathbf{u} is uniformly bounded-in-time in the L^2 norm (energy) and in the H^1 norm (enstrophy) for H^1 initial data, while in 3D the L^2 norm is bounded uniformly in time. The aim of this article is to develop efficient high-order accurate and long-time stable schemes that preserve the uniform-in-time estimates of \mathbf{u} .

Email addresses: daozhiha@buffalo.edu (Daozhi Han), wxm@eitech.edu.cn (Xiaoming Wang)

The NSE is known for displaying chaotic and turbulent behavior [5, 26, 4, 20, 21] in the forced case at large Reynolds number. The long time dynamics could be highly non-trivial exhibiting intricate intermittent behavior even at relatively small Reynolds numbers with a simple Kolmogorov forcing [2]. In the 2D case there exists a global attractor and invariant measures to the NSE, and it is understood that the long-time dynamics characterized by the global attractor and invariant measures are critical to the understanding of chaos and turbulence. To numerically capture the long-time dynamics in terms of convergence of attractors and invariant measures, it is highly desirable that the numerical schemes are efficient, high-order accurate and appropriately preserve the dissipativity of the NSE (hence long-time stable). Indeed, it is shown in [29] that dissipativity-preserving is key for a first-order in time scheme to capture the long-time statistics of a dissipative dynamical system in the sense of convergence of the underlying invariant measures.

Early works focus on fully implicit discretizations of the NSE which naturally preserve the uniform-in-time estimate of the continuous solution in the energy norm in both 2D and 3D [11, 28, 27]. Global in time error estimate is generally not expected due to the chaotic and turbulent behavior of the NSE. Under the assumption that the continuous solution of the NSE is exponentially stable, global-in-time error estimates of the Crank-Nicolson scheme were established in [11] where the discrete solution was shown to be uniformly bounded in time in the H^1 norm, and in the H^2 norm with a time-step constraint. Under time-step constraints the authors in [28, 27] proved long-time stability in the H^1 norm for the Backward Euler scheme and the Crank-Nicolson scheme, respectively. Another popular family of time-marching schemes for the NSE is the implicit-explicit discretization scheme (IMEX) where the nonlinear advection term is treated semi-explicitly and the viscous term is discretized implicitly, so as to achieve unconditional long-time stability while maintaining reasonable efficiency for long-time simulations. A general class of IMEX schemes including the fractional-step methods were considered in [25] and the large-time stability in the energy norm was shown. For the 2D NSE in the vorticity-velocity formulation the authors in [10] obtained the unconditional uniform-in-time estimate in the H^1 norm for the IMEX BDF2 scheme. Recently such an estimate has also been proven for the IMEX BDF2 scheme applied directly to the 2D NSE in the primitive form, albeit with a mild time-step constraint independent of the spatial resolution [22]. See also [12] for a study on the same scheme, but in the fully discretized setting. We would like to point out that the semi-implicit treatment of the advection term utilized in the IMEX schemes mentioned above leads to the need to solve a non-symmetric, non-constant coefficient linear problem at each time step.

From efficiency standpoint it is advantageous to discretize the nonlinear advection term fully explicitly so that the same coefficient matrix is shared throughout the time-marching for long-time simulations. For the 2D NSE in the vorticity-streamfunction formulation equipped with periodic boundary condition, long-time stability in the L^2 and H^1 norms and convergence of attractors and invariant measures at vanishing

time step were proven for the first-order IMEX scheme in [8]. Subsequently the analysis was carried out for the IMEX-BDF2 scheme in [30] where the author further established the uniform in time H^2 estimate as well as convergence of the marginal distributions of the invariant measures of the scheme to those of the NSE at vanishing time-step. Note that these results are restricted to the periodic boundary case and subject to a time-step constraint of the form $k \leq CRe^{-\alpha}$, $\alpha \geq 1$ independent of spatial resolution. It can be restrictive for large Reynolds number for capturing long time dynamics.

In recent years a Lagrange multiplier type approach, termed as the Scalar Auxiliary Variable method (SAV), has been developed for solving PDEs with a gradient flow structure [23, 24], see also [9, 36, 35, 34] for early variants of this method. High order SAV methods are constructed in [1, 7, 13, 14, 32]. More recently, the SAV approach has been extended to treat the NSE and related fluid models, see for instance [19, 17, 18, 15, 3] among many others. In particular, the advective term of the NSE is treated explicitly in a SAV method and a prefactor (a scalar variable) is discretized implicitly. As a result, the SAV methods lead to the same Stokes solver across the time iterations. In the absence of an external forcing, it was shown that the SAV methods for the NSE are unconditionally stable in the sense that a (modified) energy is non-increasing, see [18] and the references cited above. In the case of linear advection diffusion equation with constant coefficient, the stability of SAV method could be attributed to the reduction of the effective Peclet number. For fixed final time and with an external forcing, the SAV methods designed in [17, 33] are also unconditionally stable. To our knowledge there are no existing SAV methods for the NSE that can preserve the uniform in time estimate of the velocity in the energy norm, and long-time estimate in the H^1 norm in the 2D case in the presence of external forcing.

In this article we propose a novel SAV method based on the second-order backward differentiation formula (SAV-BDF2) for the NSE. Unlike previous SAV methods, our equation for the auxiliary scalar variable is damped, forced, and autonomous. For external forcing bounded uniformly in time, long-time stability bound in the L^2 norm is established for the new SAV-BDF2 methods in both 2D and 3D. Furthermore, in the case of the 2D NSE in the vorticity-streamfunction formulation, it is shown that the discrete enstrophy and the H^1 norm of the vorticity are all bounded uniformly in time. When the external forcing is independent of time (autonomous), these uniform-in-time estimate, as well as the autonomous treatment of the auxiliary variable, may imply the existence of discrete global attractors to the dynamical system on the product space. Convergence of global attractors and invariant measures will be pursued in a separate work. It should be emphasized that the SAV-BDF2 methods render the same Brinkman equations or the Helmholtz equation in the 2D case at each time step. Therefore it is highly efficient for long-time computation. As far as we know the novel uniform-in-time SAV-BDF2 methods are so far the only methods that treat the nonlinear advection term of the NSE explicitly while preserving the uniform in time estimates without any time-step restriction in the presence of external forcing.

The rest of the article is organized as follows. In Sec. 2 the general scheme and the scheme for 2D NSE

in streamline formulation are introduced, and the long-time stability of the schemes are established. Error analysis for the general scheme in 2D is performed in Sec. 2.2. Numerical results related to accuracy, stability and robustness of the proposed methods are reported in Sec. 4. Some concluding remarks are provided in Sec. 5.

2. The numerical scheme

2.1. The general scheme

One first introduces a scalar auxiliary variable (SAV) $q(t)$ such that

$$\frac{dq}{dt} + \gamma q - \int_{\Omega} (\mathbf{u} \cdot \nabla) \mathbf{u} \cdot \mathbf{u} \, dx = \gamma, \quad q(0) = 1, \quad (2.1)$$

where $\gamma > 0$ is a user-specified free parameter. It is noted that $q(t) \equiv 1$. One then writes the NSe (1.1) as an expanded system

$$\frac{\partial \mathbf{u}}{\partial t} + q(t) \mathbf{u} \cdot \nabla \mathbf{u} - \frac{1}{Re} \Delta \mathbf{u} = -\nabla p + \mathbf{F}, \quad \nabla \cdot \mathbf{u} = 0, \quad (2.2)$$

$$\frac{dq}{dt} + \gamma q - \int_{\Omega} (\mathbf{u} \cdot \nabla) \mathbf{u} \cdot \mathbf{u} \, dx = \gamma. \quad (2.3)$$

Let $k > 0$ be the time step size, $t^n = nk$ for an integer n , and denote the numerical approximation of \mathbf{u} at t^n by \mathbf{u}^n . The second order backward differentiation (BDF2) approximation of the derivative is then defined as

$$\delta_t \mathbf{u}^{n+1} := \frac{3\mathbf{u}^{n+1} - 4\mathbf{u}^n + \mathbf{u}^{n-1}}{2k}. \quad (2.4)$$

Furthermore, the extrapolated approximation is denoted by $\bar{\mathbf{u}}^{n+1} := 2\mathbf{u}^n - \mathbf{u}^{n-1}$. Finally, the generalized G matrix is defined as

$$G := \frac{1}{4} \begin{bmatrix} 1 & -2 \\ -2 & 5 \end{bmatrix}, \quad (2.5)$$

and the associated (generalized) G -norm is defined as $\|\mathbf{V}\|_G := \mathbf{V} \cdot G \mathbf{V}$ where \mathbf{V} has two entries of either vectors or scalars. Recall the equivalency between the G -norms and standard norms

$$c_l \|\mathbf{V}\|_G^2 \leq \|\mathbf{V}\|^2 \leq c_u \|\mathbf{V}\|_G^2, \quad (2.6)$$

$$c_l |Q|_G^2 \leq |Q|^2 \leq c_u |Q|_G^2, \quad (2.7)$$

where c_l, c_u are positive constants.

We also assume that the boundary conditions ensure the validity of the Poincaré's inequality, i.e., there exists c_0 such that $\|\nabla \mathbf{u}\|^2 \geq c_0 \|\mathbf{u}\|^2$.

Applying the modified BDF2 algorithm to the system (2.2)–(2.3), one derives the BDF2-SAV scheme as follows

$$\delta_t \mathbf{u}^{n+1} + \frac{1}{Re} \Delta \mathbf{u}^{n+1} + q^{n+1} (\bar{\mathbf{u}}^{n+1} \cdot \nabla) \bar{\mathbf{u}}^{n+1} + \nabla p^{n+1} = \mathbf{F}^{n+1}, \quad \nabla \cdot \mathbf{u}^{n+1} = 0, \quad (2.8)$$

$$\delta_t q^{n+1} + \gamma q^{n+1} - \int_{\Omega} (\bar{\mathbf{u}}^{n+1} \cdot \nabla) \bar{\mathbf{u}}^{n+1} \cdot \mathbf{u}^{n+1} dx = \gamma. \quad (2.9)$$

Before establishing the long-time stability of the algorithm, one comments on how to solve the linear system. In light of the linearity one performs a linear superposition by setting

$$\mathbf{u}^{n+1} = \mathbf{u}_1 + q^{n+1} \mathbf{u}_2, \quad p^{n+1} = p_1 + q^{n+1} p_2,$$

where (\mathbf{u}_i, p_i) satisfies the Brinkman-type equations

$$\frac{3\mathbf{u}_i}{2k} + \frac{1}{Re} \Delta \mathbf{u}_i + \nabla p_i = \mathbf{f}_i, \quad \nabla \cdot \mathbf{u}_i = 0,$$

with

$$\mathbf{f}_1 := \mathbf{F}^{n+1} + \frac{4\mathbf{u}^n - \mathbf{u}^{n-1}}{2k}; \quad \mathbf{f}_2 := -(2\mathbf{u}^n - \mathbf{u}^{n-1}) \cdot \nabla (2\mathbf{u}^n - \mathbf{u}^{n-1}). \quad (2.10)$$

Once \mathbf{u}_1 and \mathbf{u}_2 are available, one updates q^{n+1} from the linear scalar Eq. (2.9). The scheme is highly efficient because it is linear and the positive coefficient matrix does not change in time.

Theorem 2.1. *Suppose $\mathbf{u}_0 \in \mathbf{H}_0^1(\Omega)$, $\mathbf{F} \in \mathbf{L}^\infty(0, \infty; \mathbf{L}^2(\Omega))$ and the scheme (2.8)–(2.9) is initiated by the first order counterpart. Then for any $k > 0$ the scheme (2.8)–(2.9) is long-time stable in the sense that $\|\mathbf{u}^n\| + |q^n| \leq C$ for any $n \geq 2$ where C is a constant dependent on $\|\mathbf{u}_0\|_{H^1}$ and $\|\mathbf{F}\|_{L^\infty(0, \infty; L^2(\Omega))}$.*

Proof. Testing Eq. (2.8) with $\mathbf{u}^{n+1}k$, multiplying Eq. (2.9) by $q^{n+1}k$, and taking summation of the resultants, one obtains

$$\begin{aligned} & (\|\mathbf{V}^{n+1}\|_G^2 + |Q^{n+1}|_G^2) - (\|\mathbf{V}^n\|_G^2 + |Q^n|_G^2) + \frac{1}{4} \|\mathbf{u}^{n+1} - 2\mathbf{u}^n + \mathbf{u}^{n-1}\|^2 + \frac{1}{4} |q^{n+1} - 2q^n + q^{n-1}|^2 \\ & + \frac{k}{Re} \|\nabla \mathbf{u}^{n+1}\|^2 + k\gamma |q^{n+1}|^2 \leq \frac{c_0}{2Re} k \|\mathbf{u}^{n+1}\|^2 + \frac{kRe}{2c_0} \|\mathbf{F}\|^2 + \frac{k\gamma}{2} |q^{n+1}|^2 + \frac{k\gamma}{2}. \end{aligned} \quad (2.11)$$

which simplifies to

$$(\|\mathbf{V}^{n+1}\|_G^2 + |Q^{n+1}|_G^2) + \frac{c_0}{4Re} k \|\mathbf{u}^{n+1}\|^2 + \frac{k\gamma}{2} |q^{n+1}|^2 \leq (\|\mathbf{V}^n\|_G^2 + |Q^n|_G^2) + \frac{Rek}{2c_0} \|\mathbf{F}\|^2 + \frac{k\gamma}{2}. \quad (2.12)$$

Recall the equivalence of norms in (2.6) and (2.7). Let

$$0 < \beta \leq \min\left\{\frac{c_0}{8Re}, \frac{\gamma}{4}\right\}. \quad (2.13)$$

Adding $\beta k(\|\mathbf{u}^n\|^2 + |q^n|^2)$ to both sides of (2.12) yield

$$\begin{aligned} & (\|\mathbf{V}^{n+1}\|_G^2 + |Q^{n+1}|_G^2)(1 + \beta c_l k) + \frac{c_0}{8Re} k \|\mathbf{u}^{n+1}\|^2 + \frac{k\gamma}{4} |q^{n+1}|^2 \leq (\|\mathbf{V}^n\|_G^2 + |Q^n|_G^2) \\ & + \beta k(\|\mathbf{u}^n\|^2 + |q^n|^2) + \frac{Rek}{2c_0} \|\mathbf{F}\|^2 + \frac{k\gamma}{2} \end{aligned} \quad (2.14)$$

Define

$$E^n := \|\mathbf{V}^n\|_G^2 + |Q^n|_G^2 + \beta k(\|\mathbf{u}^n\|^2 + |q^n|^2). \quad (2.15)$$

Further imposing

$$(1 + \beta c_l k)\beta \leq \min\left\{\frac{c_0}{8Re}, \frac{\gamma}{4}\right\}, \quad (2.16)$$

one obtains

$$E^{n+1}(1 + \beta c_l k) \leq E^n + \frac{Rek}{2c_0} \|\mathbf{F}\|^2 + \frac{k\gamma}{2}. \quad (2.17)$$

In light of the uniform-in-time boundedness of F , it follows that

$$E^{n+1} \leq \frac{1}{(1 + \beta c_l k)^n} E^1 + \frac{1}{2\beta c_l} \left(\frac{Re}{c_0} \|\mathbf{F}\|_{L^\infty(0, \infty; L^2(\Omega))}^2 + \gamma \right), \quad n = 2, 3, \dots \quad (2.18)$$

This completes the proof. \square

Assuming $k \leq 1$, one can choose the largest β such that

$$0 < \beta \leq \min\left\{\frac{c_0}{8Re}, \frac{\gamma}{4}\right\}, \quad (1 + \beta c_l)\beta \leq \min\left\{\frac{c_0}{8Re}, \frac{\gamma}{4}\right\}. \quad (2.19)$$

The estimate (2.18) then implies

$$\limsup_{n \rightarrow \infty} E^n \leq \frac{1}{2\beta c_l} \left(\frac{Re}{c_0} \|\mathbf{F}\|_{L^\infty(0, \infty; L^2(\Omega))}^2 + \gamma \right) := R_0^2. \quad (2.20)$$

Corollary 2.1. *For $k \leq 1$ and $\|\mathbf{F}\|_{L^\infty(0, \infty; L^2(\Omega))} \leq C$, there exists an absorbing ball of radius R_0 to the scheme (2.8)–(2.9). In particular, if F is independent of time, the scheme (2.8)–(2.9) generates a discrete dissipative dynamical system with an absorbing ball on the product space $(\mathbb{H} \times \mathbb{R})^2$.*

Remark 2.1. *One solves Eq. (2.2) exactly to find*

$$q(t) = 1 + \int_0^t e^{-\gamma(t-s)} \int_\Omega (\mathbf{u} \cdot \nabla) \mathbf{u} \cdot \mathbf{u} \, dx ds.$$

In the discrete case (2.9), a larger γ would reduce the error associated with the discretization of the advection term. In the limit $\gamma \rightarrow \infty$, $q \equiv 1$, which would eliminate the effect of q and the scheme would be conditionally stable. In the numerical tests we choose $\gamma = 1000$.

Remark 2.2. *It is clear that the FSAV-BDF2 scheme is applicable to a general class of forced dissipative dynamical system identified in [31]:*

$$\frac{d\mathbf{u}}{dt} + A\mathbf{u} + N(\mathbf{u}, \mathbf{u}) = \mathbf{F}(t), \quad \mathbf{u}|_{t=0} = \mathbf{u}_0,$$

where A is a positive symmetric linear operator, N is nonlinear and skew-symmetric, $N(\mathbf{u}, \mathbf{u}) \cdot \mathbf{u} = 0$, and $\mathbf{F} \in \mathbf{L}^\infty(0, \infty; \mathbf{L}^2(\Omega))$. The FSAV-BDF2 scheme then reads

$$\delta_t \mathbf{u}^{n+1} + A\mathbf{u}^{n+1} + q^{n+1} N(2\mathbf{u}^n - \mathbf{u}^{n-1}, 2\mathbf{u}^n - \mathbf{u}^{n-1}) = \mathbf{F}^{n+1}, \quad (2.21)$$

$$\delta_t q^{n+1} + \gamma q^{n+1} - N(2\mathbf{u}^n - \mathbf{u}^{n-1}, 2\mathbf{u}^n - \mathbf{u}^{n-1}) \cdot \mathbf{u}^{n+1} = \gamma. \quad (2.22)$$

Following the proof of Theorem 2.1 one can show that the scheme (2.21)–(2.22) is unconditionally long-time stable.

2.2. The scheme for the 2D Navier-Stokes equations

It is known that for 2D Navier-Stokes equations the H^1 norm of the velocity field is also uniformly bounded in time if the initial data is in the same class. Here we design a BDF2-SAV method for the 2D Navier-Stokes equations in the streamline-vorticity formulation that preserves this important property. Specifically we consider the following boundary conditions

$$\mathbf{u} \cdot \mathbf{n} = 0, \quad \omega := \nabla \times \mathbf{u} = 0, \quad \text{on } \partial\Omega. \quad (2.23)$$

In the case of a simply connected domain, the 2D Navier-Stokes equations can then be written in the streamfunction-vorticity form as follows

$$\frac{\partial \omega}{\partial t} - \frac{1}{Re} \Delta \omega + \nabla^\perp \psi \cdot \nabla \omega = F, \quad \omega = -\Delta \psi, \quad (2.24)$$

$$\omega = \psi = 0, \quad \text{on } \partial\Omega. \quad (2.25)$$

The BDF2-SAV scheme for the system (2.24)–(2.25) is :

$$\delta_t \omega^{n+1} - \frac{1}{Re} \Delta \omega^{n+1} + q^{n+1} \nabla^\perp \bar{\psi}^{n+1} \cdot \nabla \bar{\omega}^{n+1} = F^{n+1}, \quad \omega^{n+1} = -\Delta \psi^{n+1}, \quad (2.26)$$

$$\delta_t q^{n+1} + \gamma q^{n+1} - \int_{\Omega} \nabla^\perp \bar{\psi}^{n+1} \cdot \nabla \bar{\omega}^{n+1} \omega^{n+1} dx = \gamma. \quad (2.27)$$

Theorem 2.2. *Suppose $\omega_0 \in H_0^1(\Omega)$, $F \in L^\infty(0, \infty; L^2(\Omega))$, and the scheme (2.26)–(2.27) is initiated by the first order counterpart. Then for $k \leq 1$, the scheme (2.26)–(2.27) is long-time stable in the sense that $\|\omega^n\|_{H^1} + \|\psi^n\|_{H^3} \leq C$ for any $n \geq 2$ where the constant C depends on $\|\omega_0\|_{H^1(\Omega)}$ and $\|F\|_{L^\infty(0, \infty; L^2(\Omega))}$.*

Proof. The proof for L^2 norm is the same as in Theorem 2.1. For the H^1 estimate, we test Eq. (2.26) by $-k\Delta\omega$ and perform integration by parts

$$\begin{aligned} & \|\nabla V^{n+1}\|_G^2 - \|\nabla V^n\|_G^2 + \frac{1}{4} \|\nabla(\omega^{n+1} - 2\omega^n + \omega^{n-1})\|^2 + \frac{k}{Re} \|\Delta\omega^{n+1}\|^2 \\ & \leq \frac{k}{4Re} \|\Delta\omega^{n+1}\|^2 + kRe \|\mathbf{F}\|^2 + kq^{n+1} \int_{\Omega} \nabla^\perp \bar{\psi}^{n+1} \cdot \nabla \bar{\omega}^{n+1} \Delta\omega^{n+1} dx. \end{aligned} \quad (2.28)$$

One controls the trilinear term as follows

$$\begin{aligned} & \left| q^{n+1} \int_{\Omega} \nabla^\perp \bar{\psi}^{n+1} \cdot \nabla \bar{\omega}^{n+1} \omega^{n+1} dx \right| \leq |q^{n+1}| \|\Delta\omega^{n+1}\| \|\nabla^\perp \bar{\psi}^{n+1}\|_{L^4} \|\nabla \bar{\omega}^{n+1}\|_{L^4} \\ & \leq C |q^{n+1}| \cdot \|\Delta\omega^{n+1}\| (\|\omega^n\| + \|\omega^{n-1}\|) \|\nabla(2\omega^n - \omega^{n-1})\|^{\frac{1}{2}} \|\Delta(2\omega^n - \omega^{n-1})\|^{\frac{1}{2}} \\ & \leq C |q^{n+1}| \cdot \|\Delta\omega^{n+1}\| (\|\omega^n\| + \|\omega^{n-1}\|) \|(2\omega^n - \omega^{n-1})\|^{\frac{1}{4}} \|\Delta(2\omega^n - \omega^{n-1})\|^{\frac{3}{4}} \\ & \leq C \|\Delta\omega^{n+1}\| (\|\omega^n\| + \|\omega^{n-1}\|)^{\frac{5}{4}} (\|\Delta\omega^n\| + \|\Delta\omega^{n-1}\|)^{\frac{3}{4}} \\ & \leq \frac{1}{4Re} \|\Delta\omega^{n+1}\|^2 + \epsilon \|\Delta\omega^n\|^2 + \epsilon \|\Delta\omega^{n-1}\|^2 + C(\epsilon) |q^{n+1}|^8 (\|\omega^n\| + \|\omega^{n-1}\|)^{10}. \end{aligned} \quad (2.29)$$

It follows that

$$\|\nabla V^{n+1}\|_G^2 - \|\nabla V^n\|_G^2 + \frac{1}{4} \|\nabla(\omega^{n+1} - 2\omega^n + \omega^{n-1})\|^2 + \frac{k}{2Re} \|\Delta\omega^{n+1}\|^2$$

$$\leq k\epsilon(\|\Delta\omega^n\|^2 + \|\Delta\omega^{n-1}\|^2) + k\left(C(\epsilon)|q^{n+1}|^8(\|\omega^n\| + \|\omega^{n-1}\|)^{10} + Re\|\mathbf{F}\|^2\right). \quad (2.30)$$

Since there exists a constant $\Lambda_1 > 0$ such that $\|\Delta\omega\|^2 \geq \Lambda_1\|\nabla\omega\|^2, \forall \omega \in H^2(\Omega) \cap H_0^1(\Omega)$, one has for any $\alpha \in (0, \frac{1}{2})$

$$\frac{k}{2Re}\|\Delta\omega^{n+1}\|^2 \geq \frac{k}{Re}\left(\frac{1}{2} - \alpha\right)\|\Delta\omega^{n+1}\|^2 + \frac{k}{Re}\alpha\Lambda_1\|\nabla\omega^{n+1}\|^2, \quad (2.31)$$

hence

$$\begin{aligned} & \|\nabla V^{n+1}\|_G^2 + \frac{k}{Re}\alpha\Lambda_1\|\nabla\omega^{n+1}\|^2 + k\theta_1\|\nabla\omega^n\|^2 + \frac{k}{Re}\left(\frac{1}{2} - \alpha\right)\|\Delta\omega^{n+1}\|^2 + \theta_2k\|\Delta\omega^n\|^2 \\ & \leq \|\nabla V^n\|_G^2 + k\theta_1\|\nabla\omega^n\|^2 + k(\epsilon + \theta_2)\|\Delta\omega^n\|^2 + \epsilon k\|\Delta\omega^{n-1}\|^2 \\ & \quad + k\left(C(\epsilon)|q^{n+1}|^8(\|\omega^n\| + \|\omega^{n-1}\|)^{10} + Re\|\mathbf{F}\|^2\right), \end{aligned} \quad (2.32)$$

for any $\theta_1, \theta_2 > 0$.

One now defines

$$E^n := \|\nabla V^n\|_G^2 + k\theta_1\|\nabla\omega^n\|^2 + k\theta_3\|\nabla\omega^{n-1}\|^2 + k(\epsilon + \theta_2)\|\Delta\omega^n\|^2 + \epsilon k\|\Delta\omega^{n-1}\|^2, \quad (2.33)$$

with $\theta_3 > 0$ to be determined. Provided that $k \leq 1$ and

$$\frac{\beta}{c_i} + (1 + \beta)\theta_1 \leq \frac{\alpha\Lambda_1}{Re}, \quad (2.34)$$

$$\frac{\beta}{c_i} + (1 + \beta)\theta_3 \leq \theta_1, \quad (2.35)$$

one obtains

$$\begin{aligned} & \frac{k}{Re}\alpha\Lambda_1\|\nabla\omega^{n+1}\|^2 + k\theta_1\|\nabla\omega^n\|^2 \\ & \geq \beta k\|\nabla V^{n+1}\|^2 + (1 + \beta k)\left(\theta_1k\|\nabla\omega^{n+1}\|^2 + \theta_3k\|\nabla\omega^n\|^2\right). \end{aligned} \quad (2.36)$$

Furthermore, if

$$(1 + \beta)(\epsilon + \theta_2) \leq \frac{1}{Re}\left(\frac{1}{2} - \alpha\right), \quad (2.37)$$

$$(1 + \beta)\epsilon \leq \theta_2, \quad (2.38)$$

then the inequality (2.32) becomes

$$(1 + \beta k)E^{n+1} \leq E^n + k\left(C(\epsilon)|q^{n+1}|^8(\|\omega^n\| + \|\omega^{n-1}\|)^{10} + Re\|\mathbf{F}\|^2\right). \quad (2.39)$$

The constraints (2.34), (2.35), (2.37) and (2.38) can always be fulfilled since there are six free parameters. By the uniform in time bounds in the L^2 norm, it follows $E^n \leq C, n = 2, 3, \dots$. The elliptic regularity theory further implies $\|\psi^n\|_{H^3} \leq C$. This completes the proof. \square

Remark 2.3. *The doubly periodic case can be handled in exactly the same way after we separate the average of the vorticity field. Notice that the mean of the vorticity is an invariant of the dynamics assuming the external forcing is mean-zero. The average of the vorticity contains a linear growth term if the average of the external forcing term is non-zero. Once we focus on the fluctuation (mean-zero) part, we can apply the Poincaré -Wirtinger inequality instead of the classical Poincaré inequality.*

3. Error analysis

One performs the error analysis of the general scheme (2.8)–(2.9) for a fixed final time $T > 0$. It should be noted that long-time convergence of the numerical solutions is generally not expected due to the chaotic and turbulent behavior of the NSE. For brevity, here one only considers the temporal discretization and focuses on the analysis of the scheme in 2D. The corresponding result in 3D would be local-in-time. The analysis is mostly standard, cf. [18].

Recall the vector space $\mathbf{V} := \{\mathbf{v} \in \mathbf{H}_0^1(\Omega), \nabla \cdot \mathbf{v} = 0\}$. For simplicity we suppress the spatial variables in the notation of \mathbf{u} and p , that is, $\mathbf{u}(t^n) = \mathbf{u}(t^n, \cdot)$ and $p(t^n) = p(t^n, \cdot)$. We emphasize here that $q(t) \equiv 1$. Denote the error functions by

$$e_{\mathbf{u}}^n := \mathbf{u}^n - \mathbf{u}(t^n); \quad e_p^n := p^n - p(t^n); \quad e_q^n := q^n - q(t^n) = q^n - 1. \quad (3.1)$$

We also follow the convention for vectors utilized in G-norm

$$e_{\mathbf{V}}^n := [e_{\mathbf{u}}^n, e_{\mathbf{u}}^{n-1}]^T; \quad e_Q^n := [e_q^n, e_q^{n-1}]^T.$$

Then the error functions satisfy the following equations

$$\delta_t e_{\mathbf{u}}^{n+1} + \frac{1}{Re} \Delta e_{\mathbf{u}}^{n+1} + \nabla e_p^{n+1} = \mathbf{u}(t^{n+1}) \cdot \nabla \mathbf{u}(t^{n+1}) - q^{n+1} \bar{\mathbf{u}}^{n+1} \cdot \nabla \bar{\mathbf{u}}^{n+1} + R_{\mathbf{u}}^{n+1}, \quad \nabla \cdot e_{\mathbf{u}}^{n+1} = 0, \quad (3.2)$$

$$\delta_t e_q^{n+1} + \gamma e_q^{n+1} = \int_{\Omega} \bar{\mathbf{u}}^{n+1} \cdot \nabla \bar{\mathbf{u}}^{n+1} \cdot \mathbf{u}^{n+1} dx - \int_{\Omega} \mathbf{u}(t^{n+1}) \cdot \nabla \mathbf{u}(t^{n+1}) \cdot \mathbf{u}(t^{n+1}) dx, \quad (3.3)$$

where $R_{\mathbf{u}}^{n+1} := \delta_t \mathbf{u}^{n+1}(\cdot) - \frac{\partial \mathbf{u}}{\partial t}(t^{n+1}, \cdot)$.

Theorem 3.1. *For the 2D NSE, assuming $\mathbf{u} \in H^3(0, T; \mathbf{H}_0^1(\Omega)) \cap H^1(0, T; \mathbf{H}^2(\Omega))$, and $p \in L^2(0, T; H^1(\Omega))$, then there holds*

$$\|e_{\mathbf{V}}^{m+1}\|_G^2 + \|e_Q^{m+1}\|_G^2 + k \sum_{n=1}^m \|\nabla e_{\mathbf{u}}^n\|^2 + k\gamma \sum_{n=1}^m |e_q^n|^2 + k \sum_{n=1}^m \|e_p^{n+1}\|_{L^2(\Omega)/R}^2 \leq Ck^4, \quad 1 \leq m \leq N-1. \quad (3.4)$$

Proof. Taking the \mathbf{L}^2 inner product of Eqs. (3.2) with $ke_{\mathbf{u}}^{n+1}$ and performing integration by parts, one obtains

$$\|e_{\mathbf{V}}^{n+1}\|_G^2 - \|e_{\mathbf{V}}^n\|_G^2 + \frac{k}{Re} \|\nabla e_{\mathbf{u}}^{n+1}\|^2 \leq k \left(\mathbf{u}(t^{n+1}) \cdot \nabla \mathbf{u}(t^{n+1}) - q^{n+1} \bar{\mathbf{u}}^{n+1} \cdot \nabla \bar{\mathbf{u}}^{n+1}, e_{\mathbf{u}}^{n+1} \right) + k \|R_{\mathbf{u}}^{n+1}\| \cdot \|e_{\mathbf{u}}^{n+1}\|. \quad (3.5)$$

Multiplying Eq. (3.3) by ke_q^{n+1} yields

$$|e_Q^{n+1}|_G^2 - |e_Q^n|_G^2 + k\gamma|e_q^{n+1}|^2 \leq ke_q^{n+1} \left\{ \int_{\Omega} (\bar{\mathbf{u}}^{n+1} \cdot \nabla) \bar{\mathbf{u}}^{n+1} \cdot \mathbf{u}^{n+1} dx - \int_{\Omega} (\mathbf{u}^{n+1} \cdot \nabla) \mathbf{u}^{n+1} \cdot \mathbf{u}^{n+1} dx \right\}. \quad (3.6)$$

In light of the fact $q(t) = 1$, one writes the first term on the right hand side of Eq. (3.5) as following

$$\begin{aligned} & \left(q(t^{n+1}) \mathbf{u}(t^{n+1}) \cdot \nabla \mathbf{u}(t^{n+1}) - q^{n+1} \bar{\mathbf{u}}^{n+1} \cdot \nabla \bar{\mathbf{u}}^{n+1}, e_{\mathbf{u}}^{n+1} \right) \\ &= \left([\mathbf{u}(t^{n+1}) - \bar{\mathbf{u}}^{n+1}] \cdot \nabla \mathbf{u}(t^{n+1}), e_{\mathbf{u}}^{n+1} \right) + \left(\bar{\mathbf{u}}^{n+1} \cdot \nabla [\mathbf{u}(t^{n+1}) - \bar{\mathbf{u}}^{n+1}], e_{\mathbf{u}}^{n+1} \right) \\ & \quad - e_q^{n+1} \left(\bar{\mathbf{u}}^{n+1} \cdot \nabla \bar{\mathbf{u}}^{n+1}, e_{\mathbf{u}}^{n+1} \right). \end{aligned} \quad (3.7)$$

Likewise the right hand side of Eq. (3.6) can be written as

$$\begin{aligned} & e_q^{n+1} \left(\bar{\mathbf{u}}^{n+1} \cdot \nabla \bar{\mathbf{u}}^{n+1}, e_{\mathbf{u}}^{n+1} \right) - e_q^{n+1} \left(\bar{\mathbf{u}}^{n+1} \cdot \nabla [\mathbf{u}(t^{n+1}) - \bar{\mathbf{u}}^{n+1}], \mathbf{u}(t^{n+1}) \right) \\ & \quad - e_q^{n+1} \left([\mathbf{u}(t^{n+1}) - \bar{\mathbf{u}}^{n+1}] \cdot \nabla (\mathbf{u}(t^{n+1}), \mathbf{u}(t^{n+1})) \right) \end{aligned} \quad (3.8)$$

Taking summation of the inequalities (3.5) and (3.6), in view of (3.7) and (3.8) one derives

$$\begin{aligned} & (\|e_{\mathbf{V}}^{n+1}\|_G^2 + |e_Q^{n+1}|_G^2) - (\|e_{\mathbf{V}}^n\|_G^2 + |e_Q^n|_G^2) + \frac{k}{Re} \| \nabla e_{\mathbf{u}}^{n+1} \|^2 + k\gamma |e_q^{n+1}|^2 \leq k \| R_{\mathbf{u}}^{n+1} \| \cdot \| e_{\mathbf{u}}^{n+1} \| \\ & + k \left([\mathbf{u}(t^{n+1}) - \bar{\mathbf{u}}^{n+1}] \cdot \nabla \mathbf{u}(t^{n+1}), e_{\mathbf{u}}^{n+1} \right) + k \left(\bar{\mathbf{u}}^{n+1} \cdot \nabla [\mathbf{u}(t^{n+1}) - \bar{\mathbf{u}}^{n+1}], e_{\mathbf{u}}^{n+1} \right) \\ & - ke_q^{n+1} \left(\bar{\mathbf{u}}^{n+1} \cdot \nabla [\mathbf{u}(t^{n+1}) - \bar{\mathbf{u}}^{n+1}], \mathbf{u}(t^{n+1}) \right) - ke_q^{n+1} \left([\mathbf{u}(t^{n+1}) - \bar{\mathbf{u}}^{n+1}] \cdot \nabla \mathbf{u}(t^{n+1}), \mathbf{u}(t^{n+1}) \right) \quad (3.9) \\ & := \sum_{i=1}^5 I_i, \end{aligned}$$

where $I_i, i = 1 \dots 5$ are the five terms on the right hand side of (3.9).

For I_1 ,

$$k \| R_{\mathbf{u}}^{n+1} \| \cdot \| e_{\mathbf{u}}^{n+1} \| \leq \epsilon \frac{k}{Re} \| \nabla e_{\mathbf{u}}^{n+1} \|^2 + C(\epsilon) k Re \| R_{\mathbf{u}}^{n+1} \|^2, \quad (3.10)$$

with $\epsilon > 0$ to be determined. By virtue of the notation in (3.1) one writes

$$\mathbf{u}(t^{n+1}) - \bar{\mathbf{u}}^{n+1} = D\mathbf{u}(t^{n+1}) - 2e_{\mathbf{u}}^n + e_{\mathbf{u}}^{n-1} \quad (3.11)$$

with $D\mathbf{u}(t^{n+1}) := \mathbf{u}(t^{n+1}) - 2\mathbf{u}(t^n) + \mathbf{u}(t^{n-1})$. Then I_2 is estimated by Hölder's inequality and the Sobolev embedding as follows

$$\begin{aligned} |I_2| & \leq Ck \| \mathbf{u}(t^{n+1}) - \bar{\mathbf{u}}^{n+1} \| \cdot \| \mathbf{u}(t^{n+1}) \|_{H^2} \cdot \| \nabla e_{\mathbf{u}}^{n+1} \| \\ & \leq \epsilon \frac{k}{Re} \| \nabla e_{\mathbf{u}}^{n+1} \|^2 + kC(\epsilon) Re \| \mathbf{u}(t^{n+1}) \|_{H^2}^2 (\| D\mathbf{u}(t^{n+1}) \|^2 + \| 2e_{\mathbf{u}}^n - e_{\mathbf{u}}^{n-1} \|^2) \\ & \leq \epsilon \frac{k}{Re} \| \nabla e_{\mathbf{u}}^{n+1} \|^2 + kC(\epsilon) Re \| \mathbf{u}(t^{n+1}) \|_{H^2}^2 (\| D\mathbf{u}(t^{n+1}) \|^2 + \| e_{\mathbf{V}}^n \|_G^2). \end{aligned} \quad (3.12)$$

By (3.11) one writes I_3 as

$$\begin{aligned} I_3 &= k\left(\bar{\mathbf{u}}^{n+1} \cdot \nabla D\mathbf{u}(t^{n+1}), e_{\mathbf{u}}^{n+1}\right) - k\left([2e_{\mathbf{u}}^n - e_{\mathbf{u}}^{n-1}] \cdot \nabla[2e_{\mathbf{u}}^n - e_{\mathbf{u}}^{n-1}], e_{\mathbf{u}}^{n+1}\right) \\ &\quad - k\left([2\mathbf{u}(t^n) - \mathbf{u}(t^{n-1})] \cdot \nabla[2e_{\mathbf{u}}^n - e_{\mathbf{u}}^{n-1}], e_{\mathbf{u}}^{n+1}\right). \end{aligned} \quad (3.13)$$

Recall the 2D Ladyzhenskaya's inequality [16]

$$\|\mathbf{u}\|_{L^4}^2 \leq 2\|\mathbf{u}\| \cdot \|\nabla\mathbf{u}\|. \quad (3.14)$$

The first term in (3.13) satisfies

$$\begin{aligned} \left|k\left(\bar{\mathbf{u}}^{n+1} \cdot \nabla D\mathbf{u}(t^{n+1}), e_{\mathbf{u}}^{n+1}\right)\right| &= \left|k\left(\bar{\mathbf{u}}^{n+1} \cdot \nabla e_{\mathbf{u}}^{n+1}, D\mathbf{u}(t^{n+1})\right)\right| \\ &\leq k\left(\|\bar{\mathbf{u}}^{n+1}\|_{L^4}\|\nabla e_{\mathbf{u}}^{n+1}\| \cdot \|D\mathbf{u}(t^{n+1})\|_{L^4}\right) \\ &\leq Ck\|\bar{\mathbf{u}}^{n+1}\|^{1/2}\|\nabla\bar{\mathbf{u}}^{n+1}\|^{1/2}\|\nabla e_{\mathbf{u}}^{n+1}\| \cdot \|D\mathbf{u}(t^{n+1})\|^{1/2}\|\nabla D\mathbf{u}(t^{n+1})\|^{1/2} \\ &\leq \epsilon\frac{k}{Re}\|\nabla e_{\mathbf{u}}^{n+1}\|^2 + C(\epsilon)kRe\|\bar{\mathbf{u}}^{n+1}\|^2\|\nabla D\mathbf{u}(t^{n+1})\|^2 + Ck\|\nabla\bar{\mathbf{u}}^{n+1}\|^2\|D\mathbf{u}(t^{n+1})\|^2. \end{aligned}$$

Likewise the second term in (3.13) has the estimate

$$\begin{aligned} \left|k\left([2e_{\mathbf{u}}^n - e_{\mathbf{u}}^{n-1}] \cdot \nabla[2e_{\mathbf{u}}^n - e_{\mathbf{u}}^{n-1}], e_{\mathbf{u}}^{n+1}\right)\right| &\leq Ck\|2e_{\mathbf{u}}^n - e_{\mathbf{u}}^{n-1}\| \cdot \|\nabla[2e_{\mathbf{u}}^n - e_{\mathbf{u}}^{n-1}]\| \cdot \|\nabla e_{\mathbf{u}}^{n+1}\| \\ &\leq \epsilon\frac{k}{Re}\|\nabla e_{\mathbf{u}}^{n+1}\|^2 + C(\epsilon)kRe\|\nabla[2e_{\mathbf{u}}^n - e_{\mathbf{u}}^{n-1}]\|^2\|e_{\mathbf{V}}^n\|_G^2. \end{aligned}$$

The third term in I_3 is estimated in the same way as (3.12). Hence

$$\begin{aligned} |I_3| &\leq 3\epsilon\frac{k}{Re}\|\nabla e_{\mathbf{u}}^{n+1}\|^2 + C(\epsilon)kRe\|\bar{\mathbf{u}}^{n+1}\|^2\|\nabla D\mathbf{u}(t^{n+1})\|^2 + Ck\|\nabla\bar{\mathbf{u}}^{n+1}\|^2\|D\mathbf{u}(t^{n+1})\|^2 \\ &\quad + C(\epsilon)kRe(\|\nabla[2e_{\mathbf{u}}^n - e_{\mathbf{u}}^{n-1}]\|^2 + \|2\mathbf{u}(t^n) - \mathbf{u}(t^{n-1})\|_{H^2}^2)\|e_{\mathbf{V}}^n\|_G^2. \end{aligned} \quad (3.15)$$

One controls I_4 as follows

$$\begin{aligned} |I_4| &\leq k|e_q^{n+1}| \left\{ \left| \left(\bar{\mathbf{u}}^{n+1} \cdot \nabla D\mathbf{u}(t^{n+1}), \mathbf{u}(t^{n+1}) \right) \right| + \left| \left(\bar{\mathbf{u}}^{n+1} \cdot \nabla(2e_{\mathbf{u}}^n - e_{\mathbf{u}}^{n-1}), \mathbf{u}(t^{n+1}) \right) \right| \right\} \\ &\leq \theta k\gamma|e_q^{n+1}|^2 + k\frac{C(\theta)}{\gamma}\|\bar{\mathbf{u}}^{n+1}\|^2\|\mathbf{u}(t^{n+1})\|_{H^2}^2\|\nabla D\mathbf{u}(t^{n+1})\|^2 + \tau k|e_Q^{n+1}|_G^2\|\nabla\bar{\mathbf{u}}^{n+1}\|^2 \\ &\quad + C(\tau)k\|\mathbf{u}(t^{n+1})\|_{H^2}^2\|e_{\mathbf{V}}^n\|_G^2, \end{aligned} \quad (3.16)$$

with $\theta, \tau > 0$ to be determined. Likewise I_5 satisfies the bound

$$\begin{aligned} |I_5| &\leq k|e_q^{n+1}| \left\{ \left| \left(D\mathbf{u}(t^{n+1}) \cdot \nabla\mathbf{u}(t^{n+1}), \mathbf{u}(t^{n+1}) \right) \right| + \left| \left([2e_{\mathbf{u}}^n - e_{\mathbf{u}}^{n-1}] \cdot \nabla\mathbf{u}(t^{n+1}), \mathbf{u}(t^{n+1}) \right) \right| \right\} \\ &\leq 2\theta k\gamma|e_q^{n+1}|^2 + k\frac{C(\theta)}{\gamma}\|\nabla\mathbf{u}(t^{n+1})\|^2\|\mathbf{u}(t^{n+1})\|_{H^2}^2(\|D\mathbf{u}(t^{n+1})\|^2 + \|e_{\mathbf{V}}^n\|_G^2). \end{aligned} \quad (3.17)$$

Taking $\epsilon = \frac{1}{10}$ and $\theta = \frac{1}{6}$, and collecting the estimates of $I_i, i = 1 \dots 5$ into (3.9), one obtains

$$(\|e_{\mathbf{V}}^{n+1}\|_G^2 + |e_Q^{n+1}|_G^2) - (\|e_{\mathbf{V}}^n\|_G^2 + |e_Q^n|_G^2) + \frac{k}{2Re}\|\nabla e_{\mathbf{u}}^{n+1}\|^2 + k\frac{\gamma}{2}|e_q^{n+1}|^2$$

$$\begin{aligned}
&\leq Ck \left\{ (Re + C(\tau) + \frac{1}{\gamma} \|\nabla \mathbf{u}(t^{n+1})\|^2) \|\mathbf{u}(t^{n+1})\|_{H^2}^2 + \|2\mathbf{u}(t^n) - \mathbf{u}(t^{n-1})\|_{H^2}^2 + \|\nabla[2e_{\mathbf{u}}^n - e_{\mathbf{u}}^{n-1}]\|^2 \right\} \|e_{\mathbf{V}}^n\|_G^2 \\
&\quad + Ck \left\{ (Re + \frac{1}{\gamma} \|\bar{\mathbf{u}}^{n+1}\|^2 + \frac{1}{\gamma} \|\nabla \mathbf{u}(t^{n+1})\|^2) \|\mathbf{u}(t^{n+1})\|_{H^2}^2 + Re \|\bar{\mathbf{u}}^{n+1}\|^2 \right\} \|\nabla D\mathbf{u}(t^{n+1})\|^2 \\
&\quad + CkRe \|R_{\mathbf{u}}^{n+1}\|^2 + \tau k |e_Q^{n+1}|_G^2 \|\nabla \bar{\mathbf{u}}^{n+1}\|^2 + Ck \|\nabla \bar{\mathbf{u}}^{n+1}\|^2 \|D\mathbf{u}(t^{n+1})\|^2. \tag{3.18}
\end{aligned}$$

Taking summation of (3.18) from $n = 1$ to $m \leq N - 1$, in light of the stability estimates of the numerical solution as well as the regularity assumption on the exact solution, one derives

$$\begin{aligned}
&(\|e_{\mathbf{V}}^{m+1}\|_G^2 + |e_Q^{n+1}|_G^2) + \frac{k}{2Re} \sum_{n=1}^m \|\nabla e_{\mathbf{u}}^{n+1}\|^2 + k \frac{\gamma}{2} \sum_{n=1}^m |e_q^{n+1}|^2 \\
&\leq C(Re, \tau, \gamma) k \sum_{n=1}^m \{1 + \|\nabla[2e_{\mathbf{u}}^n - e_{\mathbf{u}}^{n-1}]\|^2\} \|e_{\mathbf{V}}^n\|_G^2 + \tau k \sum_{n=2}^m \|\nabla \bar{\mathbf{u}}^n\|^2 |e_Q^n|_G^2 + \tau k |e_Q^{m+1}|_G^2 \|\nabla \bar{\mathbf{u}}^{m+1}\|^2 \\
&\quad + C(Re, \gamma) k \sum_{n=1}^m \|\nabla D\mathbf{u}(t^{n+1})\|^2 + C \max_{n \geq 1} \|D\mathbf{u}(t^{n+1})\|^2 \sum_{n=1}^m k \|\nabla \bar{\mathbf{u}}^{n+1}\|^2 + Re \sum_{n=1}^m \|R_{\mathbf{u}}^{n+1}\|^2 + \|e_{\mathbf{V}}^1\|_G^2. \tag{3.19}
\end{aligned}$$

Since $k \|\nabla \bar{\mathbf{u}}^{m+1}\|^2 \leq C$, one chooses the largest τ such that $\tau k \|\nabla \bar{\mathbf{u}}^{m+1}\|^2 \leq \frac{1}{2}$. The inequality (3.19) then becomes

$$\begin{aligned}
&(\|e_{\mathbf{V}}^{m+1}\|_G^2 + |e_Q^{n+1}|_G^2) + \frac{k}{Re} \sum_{n=1}^m \|\nabla e_{\mathbf{u}}^{n+1}\|^2 + k\gamma \sum_{n=1}^m |e_q^{n+1}|^2 \\
&\leq C(Re, \gamma) k \sum_{n=1}^m \{1 + \|\nabla[2e_{\mathbf{u}}^n - e_{\mathbf{u}}^{n-1}]\|^2\} \|e_{\mathbf{V}}^n\|_G^2 + \tau k \sum_{n=2}^m \|\nabla \bar{\mathbf{u}}^n\|^2 |e_Q^n|_G^2 + Ck^4. \tag{3.20}
\end{aligned}$$

An application of the discrete Gronwall's inequality implies

$$(\|e_{\mathbf{V}}^{m+1}\|_G^2 + |e_Q^{n+1}|_G^2) + \frac{k}{Re} \sum_{n=1}^m \|\nabla e_{\mathbf{u}}^{n+1}\|^2 + k\gamma \sum_{n=1}^m |e_q^{n+1}|^2 \leq C(Re, \gamma) k^4. \tag{3.21}$$

The error estimate for pressure is standard, cf. [6]. Since the divergence operator is an isomorphism from \mathbf{V}^\perp onto $L^2(\Omega)/R$, there exist $\mathbf{v}^{n+1} \in \mathbf{H}_0^1(\Omega)$ such that

$$-\nabla \cdot \mathbf{v}^{n+1} = e_p^{n+1}, \quad \|\nabla \mathbf{v}^{n+1}\| \leq C \|e_p^{n+1}\|_{L^2(\Omega)/R}.$$

Then it follows from the error equations (3.2) that

$$\begin{aligned}
&\|e_p^{n+1}\|_{L^2(\Omega)/R}^2 = (\nabla e_p^{n+1}, \mathbf{v}^{n+1}) \\
&\leq \|\nabla e_{\mathbf{u}}^{n+1}\| \cdot \|\nabla \mathbf{v}^{n+1}\| + \|R_{\mathbf{u}}^{n+1}\| \cdot \|\mathbf{v}^{n+1}\| + \left| ([\mathbf{u}(t^{n+1}) - \bar{\mathbf{u}}^{n+1}] \cdot \nabla \mathbf{u}(t^{n+1}), \mathbf{v}^{n+1}) \right| \\
&\quad + \left| (\bar{\mathbf{u}}^{n+1} \cdot \nabla [\mathbf{u}(t^{n+1}) - \bar{\mathbf{u}}^{n+1}], \mathbf{v}^{n+1}) \right| + \left| e_q^{n+1} (\bar{\mathbf{u}}^{n+1} \cdot \nabla \bar{\mathbf{u}}^{n+1}, \mathbf{v}^{n+1}) \right| \\
&\leq C(\|\nabla e_{\mathbf{u}}^{n+1}\| + \|R_{\mathbf{u}}^{n+1}\|) \|\nabla \mathbf{v}^{n+1}\| + (\|\nabla D\mathbf{u}(t^{n+1})\| + \|\nabla(2e_{\mathbf{u}}^n - e_{\mathbf{u}}^{n-1})\|) \|\nabla \mathbf{u}(t^{n+1})\| \cdot \|\nabla \mathbf{v}^{n+1}\| \\
&\quad + C \|\bar{\mathbf{u}}^{n+1}\|^{1/2} \|\nabla \bar{\mathbf{u}}^{n+1}\|^{1/2} \|\nabla \mathbf{v}^{n+1}\| (\|\mathbf{u}(t^{n+1})\|^{1/2} \|\nabla D\mathbf{u}(t^{n+1})\|^{1/2} + \|2e_{\mathbf{u}}^n - e_{\mathbf{u}}^{n-1}\|^{1/2} \|\nabla(2e_{\mathbf{u}}^n - e_{\mathbf{u}}^{n-1})\|^{1/2}) \\
&\quad + C |e_q^{n+1}| \cdot \|\bar{\mathbf{u}}^{n+1}\| \cdot \|\nabla \bar{\mathbf{u}}^{n+1}\| \cdot \|\nabla \mathbf{v}^{n+1}\|, \tag{3.22}
\end{aligned}$$

where integration by parts and Ladyzhenskaya's inequality (3.14) have been utilized in the estimate of the trilinear terms. It follows that

$$\begin{aligned} \|e_p^{n+1}\|_{L^2(\Omega)/R} &\leq C(\|\nabla e_{\mathbf{u}}^{n+1}\| + \|R_{\mathbf{u}}^{n+1}\| + \|\nabla D\mathbf{u}(t^{n+1})\| + \|\nabla(2e_{\mathbf{u}}^n - e_{\mathbf{u}}^{n-1})\|) + C|e_q^{n+1}| \cdot \|\nabla \bar{\mathbf{u}}^{n+1}\| \\ &+ C\|\nabla \bar{\mathbf{u}}^{n+1}\|(\|D\mathbf{u}(t^{n+1})\| + \|2e_{\mathbf{u}}^n - e_{\mathbf{u}}^{n-1}\|) + \|\nabla D\mathbf{u}(t^{n+1})\| + \|\nabla(2e_{\mathbf{u}}^n - e_{\mathbf{u}}^{n-1})\|. \end{aligned} \quad (3.23)$$

Therefore

$$\begin{aligned} &k \sum_{n=1}^m \|e_p^{n+1}\|_{L^2(\Omega)/R}^2 \\ &\leq Ck \sum_{n=1}^m (\|\nabla e_{\mathbf{u}}^{n+1}\|^2 + \|R_{\mathbf{u}}^{n+1}\|^2 + \|\nabla D\mathbf{u}(t^{n+1})\|^2 + \|\nabla(2e_{\mathbf{u}}^n - e_{\mathbf{u}}^{n-1})\|^2) + C \max_{n \geq 1} |e_q^{n+1}|^2 \sum_{n=1}^m k \|\nabla \bar{\mathbf{u}}^{n+1}\|^2 \\ &+ C \sum_{n=1}^m k \|\nabla \bar{\mathbf{u}}^{n+1}\|^2 \max_{n \geq 1} (\|D\mathbf{u}(t^{n+1})\|^2 + \|2e_{\mathbf{u}}^n - e_{\mathbf{u}}^{n-1}\|^2) + \sum_{n=1}^m k (\|\nabla D\mathbf{u}(t^{n+1})\|^2 + \|\nabla(2e_{\mathbf{u}}^n - e_{\mathbf{u}}^{n-1})\|^2) \\ &\leq Ck^4. \end{aligned} \quad (3.24)$$

This completes the proof. \square

4. Numerical experiments

Numerical tests are performed to demonstrate the accuracy, efficiency and robustness of the BDF2-SAV schemes. In all tests, the scheme is initiated by a first order scheme with explicit discretization of the nonlinear term.

4.1. Accuracy

We perform three tests for verification of accuracy using manufactured solutions. In the first two tests, finite element is used for spatial discretization for the SAV-BDF2 schemes in the primitive form and the streamfunction-vorticity form, respectively. The implementation is carried out using the open-source package FreeFem++. In the first two examples, the computational domain is $\Omega = [0, 1]^2$, the final time is set at $T = 100$, h and k are simultaneously refined through the relation $h = \frac{1}{2}k$, so that the error is dominated by the temporal error.

For the SAV-BDF2 algorithm in the primitive form, The test problem is manufactured according to the exact solution

$$\begin{aligned} u_1 &= 2x^2y \sin(t)(x-1)^2(y-1)^2 + x^2y^2 \sin(t)(2y-2)(x-1)^2, \\ u_2 &= -2xy^2 \sin(t)(x-1)^2(y-1)^2 - x^2y^2 \sin(t)(2x-2)(y-1)^2, \\ p &= \cos(t)xy. \end{aligned}$$

Table 1: Relative error for \mathbf{u} and p in the L^2 norm, and error for q with $k = 2h$ and $P2 - P1$ Taylor-Hood finite element.

k	$\ e_u\ $	order	$\ e_p\ $	order	$ q - 1 $
0.5	0.0801977		0.0121033		2.47015e-09
0.25	0.0108756	2.88	0.00302578	2.00	5.91561e-11
0.125	0.00151803	2.84	0.000756443	2.00	6.28753e-12
0.0625	0.000242224	2.65	0.000189111	2.00	1.74971e-13
0.03125	4.51685e-05	2.42	4.72777e-05	2.00	2.22045e-16
0.015625	9.5513e-06	2.24	1.18194e-05	2.00	6.66134e-16
0.0078125	2.17576e-06	2.13	2.95486e-06	2.00	1.11022e-16

The parameters are $Re = 100$, $\gamma = 1000$. The Taylor-Hood $P2 - P1$ finite element pair is utilized for spatial discretization. The relative error for \mathbf{u} and p in the L^2 norm, and relative error for q are displayed in the Table 1.

For the SAV-BDF2 algorithm in the streamfunction-vorticity formulation, the true solutions are

$$\begin{aligned}\omega &= \sin(t) \sin(\pi x) \sin(2\pi y), \\ \psi &= -10 \cos(t) x(x-1) y(y-1),\end{aligned}$$

in which $Re = 10$, $\gamma = 1000$. $P2$ finite elements are utilized for both variables. The relative error for ω and ψ in the L^2 norm, and relative error for q are displayed in the Table 2.

Table 2: Relative error for ω and ψ in the L^2 norm, and error for q with $k = 2h$ and $P2 - P2$ finite element pair

k	$\ e_\omega\ $	order	$\ e_\psi\ $	order	$ q - 1 $
0.5	0.501288		0.0110108		2.47015e-09
0.25	0.098924	2.34	0.00196049	2.49	0.000131017
0.125	0.022645	2.12	0.000417379	2.23	6.81064e-06
0.0625	0.00560761	2.01	0.000100779	2.05	3.72619e-07
0.03125	0.00139695	2.00	2.49413e-05	2.01	1.0624e-09
0.015625	0.000348469	2.00	6.21157e-06	2.01	6.27696e-11
0.0078125	8.70057e-05	2.00	1.55032e-06	2.00	3.80607e-12

Since periodic boundary conditions will be used in the following for simulations of coherent structures, the SAV-BDF2 scheme in the stream function formulation is also implemented in Matlab utilizing Fourier collocation methods. The exact solutions are

$$\omega = \sin(t) \sin(2\pi x) \sin(2\pi y), \quad \psi = \cos(t) \cos(2\pi x) \cos(2\pi y).$$

The parameters are $Re = 10, \gamma = 1000, T = 100, \Omega = (0, 1)^2$. 32 Fourier modes are employed. The relative error in l^∞ norm and convergence order is displayed in Table 3.

Table 3: Relative error for ω and ψ in the l^∞ norm, and error for q with 32 Fourier modes in each direction

k	$\ e_\omega\ _\infty$	order	$\ e_\psi\ _\infty$	order	$ q - 1 $
0.05	1.36619		1.818292e-03		6.096786e-03
0.025	1.025531e-03	10.38	8.159268e-06	7.80	3.004133e-09
0.0125	2.553669e-04	2.00	2.031416e-06	2.00	6.844236e-11
0.00625	6.363869e-05	2.00	5.064025e-07	2.00	4.260259e-12
0.003125	1.588605e-05	2.00	1.264143e-07	2.00	2.654543e-13
0.0015625	3.968483e-06	2.00	3.157964e-08	2.00	1.643130e-14
0.00078125	9.917372e-07	2.00	7.891879e-09	2.00	1.110223e-15

4.2. The Kolmogorov flow

As a Benchmark test, one considers the 2D NSE with the Kolmogorov forcing and periodic boundary conditions in the domain $\Omega = (0, 2\pi)^2$, as is detailed in [2]. A typical Kolmogorov forcing takes the form

$$\mathbf{f} := \left[\frac{m^3}{Re} \cos(my), 0 \right]^T, \quad m \in \mathbb{N}^+. \quad (4.1)$$

The steady-state solution, also known as the basic Kolmogorov flow, is given in a streamfunction formulation as $\psi = \sin(my)$. The steady-state solution is stable when Re is relatively small. It becomes unstable as Re crosses a critical value and coherent structure develops. In the following simulations, the SAV-BDF2 scheme is implemented in Matlab in conjunction with the Fourier collocation method using 256 modes.

4.2.1. Long-time stability

One verifies the long-time stability of the SAV-BDF2 scheme for the 2D NSE in the stream function formulation with the Kolmogorov forcing (4.1) and $m = 2, Re = 100$. The initial stream function is a (periodic) perturbation of the steady-state solution

$$\psi(0, x, y) = \sin(2y) + 0.001 \sin(2x) \sin(2y).$$

The evolution of the L^2 norm and H^1 norm of the vorticity by the SAV-BDF2 scheme for $T = 1000$ is depicted in Fig. 1 with 256 Fourier modes and $k = 0.01, 0.005, 0.0025$ respectively. It is noted that the BDF2 IMEX scheme with explicit discretization of the advection term blows up for $k = 0.003$.

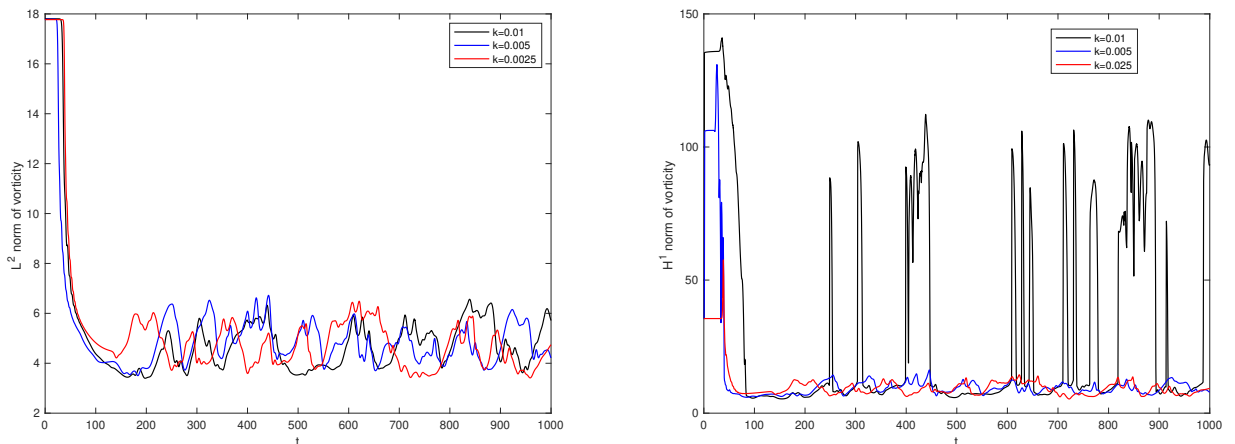


Figure 1: The L^2 norm and H^1 norm of the vorticity as a function of time by the SAV-BDF2 scheme with 256 Fourier modes and $k = 0.01, 0.005, 0.0025$ respectively.

4.2.2. Bursting

The initial condition used in this simulation is a perturbation to the basic Kolmogorov flow

$$\psi(0, x, y) = \sin(2y) + 0.001 \sin(2\pi x) \sin(2\pi y).$$

It is discovered through numerical simulation in [2] that at $Re = 25.70$ the solution is quasi-periodic which consists of a traveling structure plus additional time dependent behavior, and bursts occur intermittently at $Re \geq 25.77$. In the following simulation, the Reynolds number is taken to be 25.7715, $k = 0.001$, and the final time is $T = 10000$. Fourier collocation method is utilized for spatial discretization with 256 Fourier modes.

The real and imaginary part of the Fourier coefficient of mode e^{iy} is plotted in Fig. 2 as a function of time. Bursts occur intermittently characterized by a sudden dramatic change of magnitude of the Fourier coefficient. The evolution of the maximum vorticity and the L^2 norm of the gradient is displayed in Fig. 3, which further corroborates the appearance of bursts. The dynamics undergo a long laminar regime, then a chaotic explosion (burst) ensues, followed by another long period of laminar regime. The pattern repeats in time. It is noted in [2] that the occurrences of bursts do not correlate with each other. Fig. 4 confirms that the time interval between bursts is not constant and appears to be random. The power spectrum density of the fluctuation of the maximum vorticity is shown in Fig. 5. The wide spread of frequencies indicate non-periodic motion, while the concentration of power at low frequencies suggests the intermittency of bursting phenomenon.

A zoomed-in plot of the maximum vorticity across the bursting event between $t = 1000$ and 2000 is displayed in Fig. 6. Fig. 7 demonstrates the typical dynamics during during a bursting event. It is observed that the burst is associated with spatially localized concentration of vorticity.

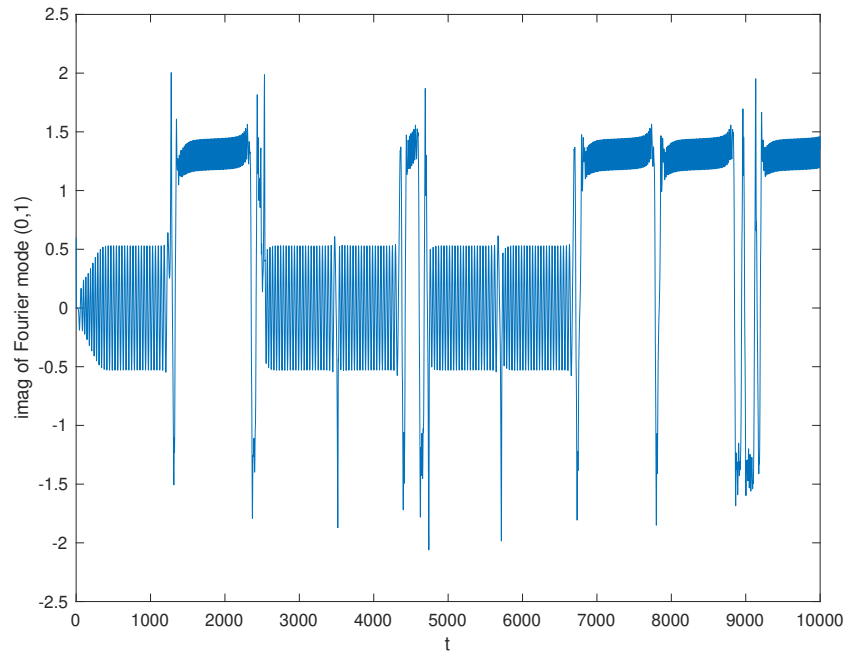
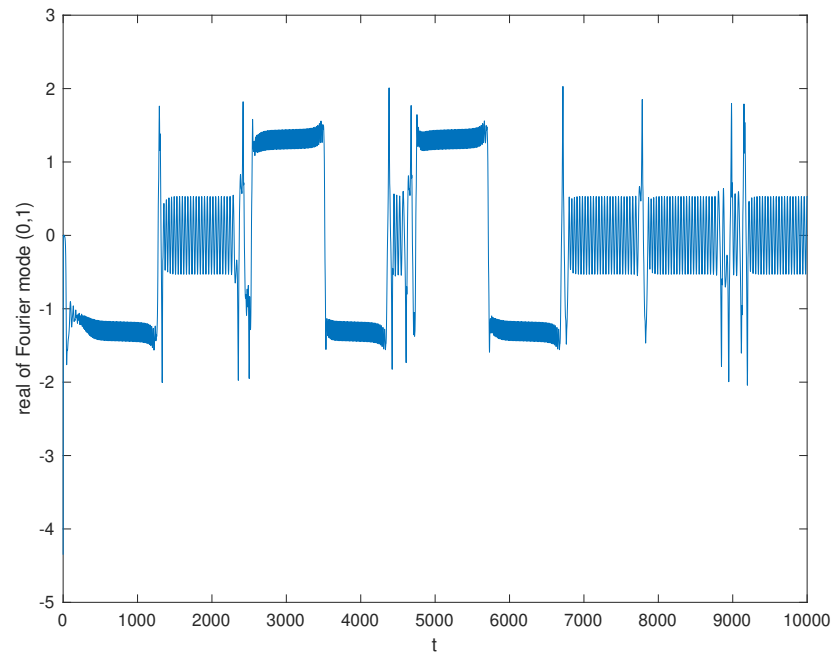


Figure 2: The real and imaginary part of the Fourier coefficient of mode e^{iy} as a function of time. $Re = 25.7715, k = 0.001$ with 256 Fourier modes.

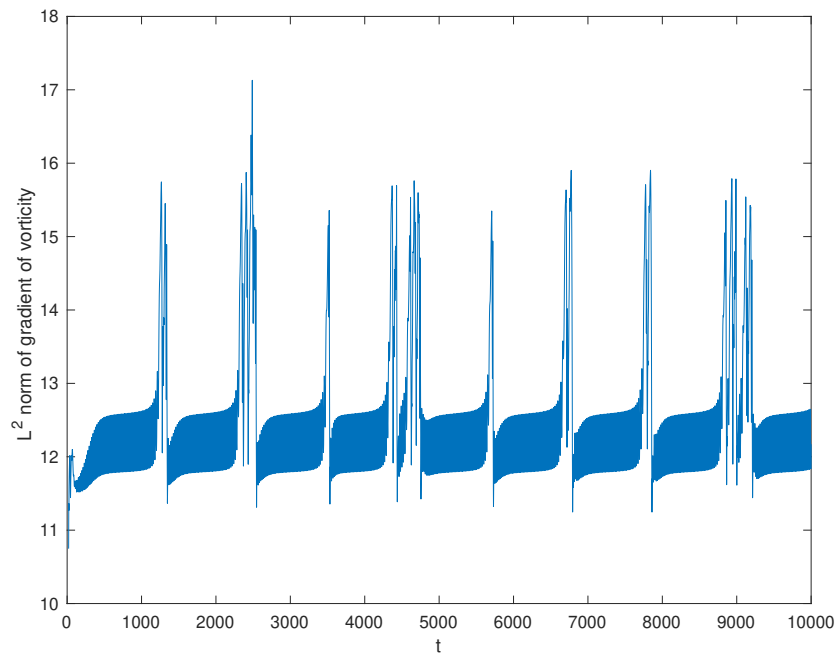
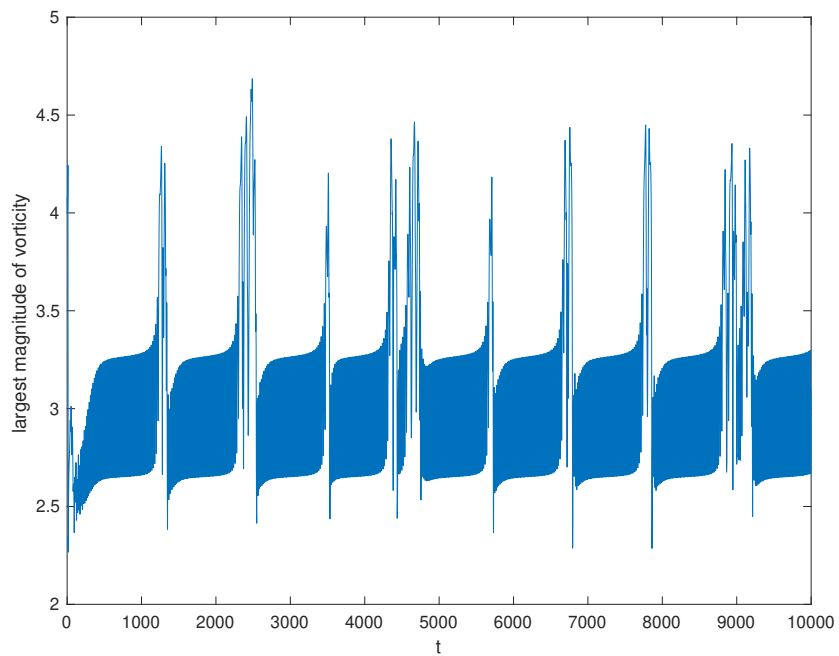


Figure 3: The largest magnitude and the L^2 norm of gradient of vorticity as a function of time. $Re = 25.7715, k = 0.001$ with 256 Fourier modes.

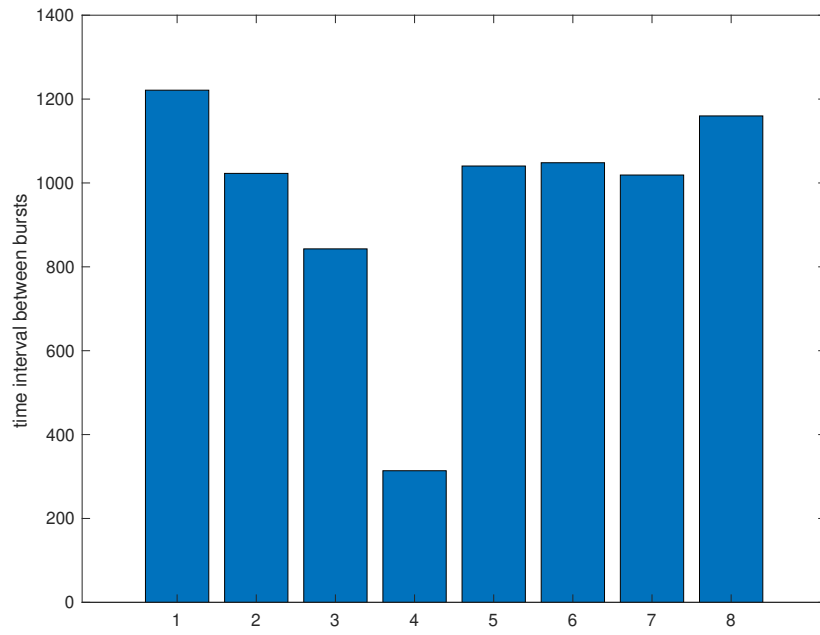


Figure 4: Time interval between bursts

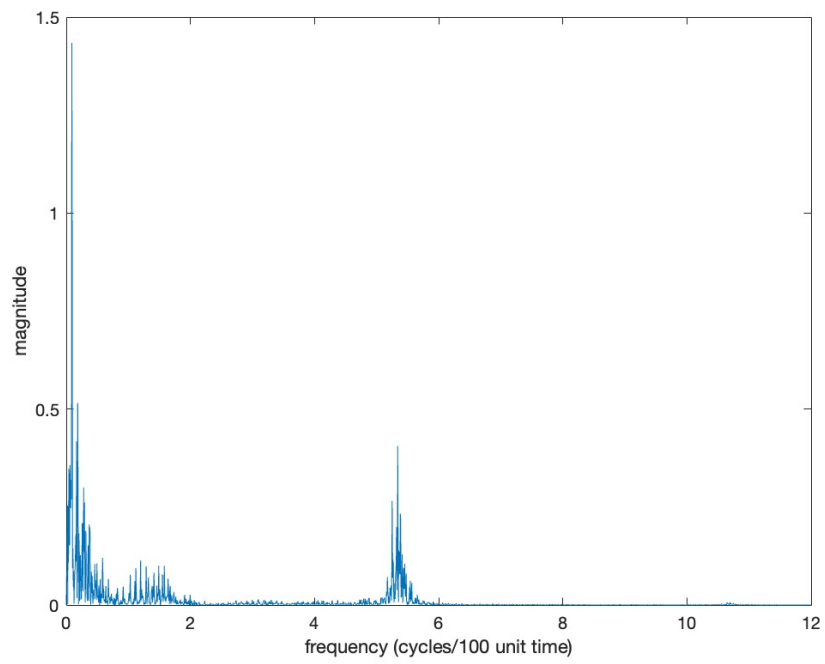


Figure 5: Power spectrum density plot

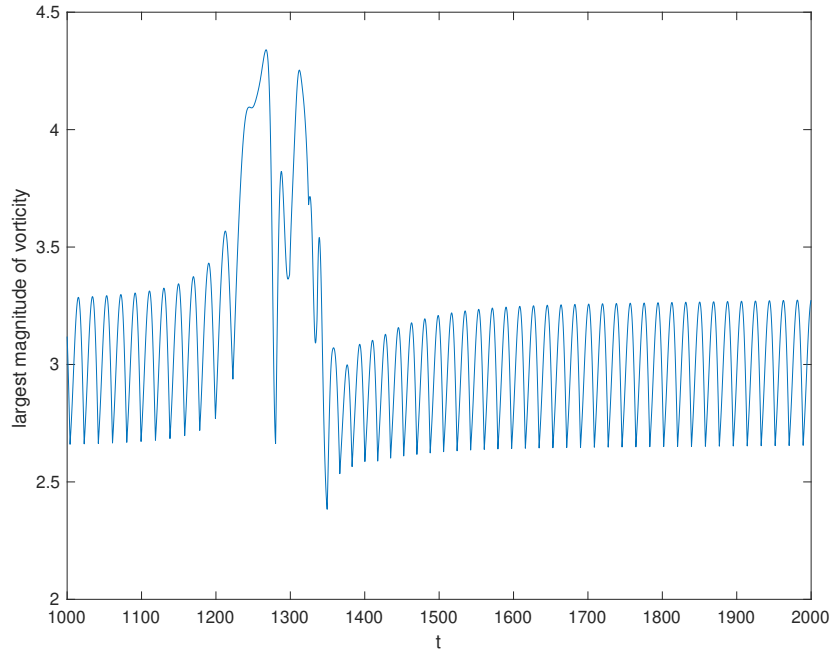


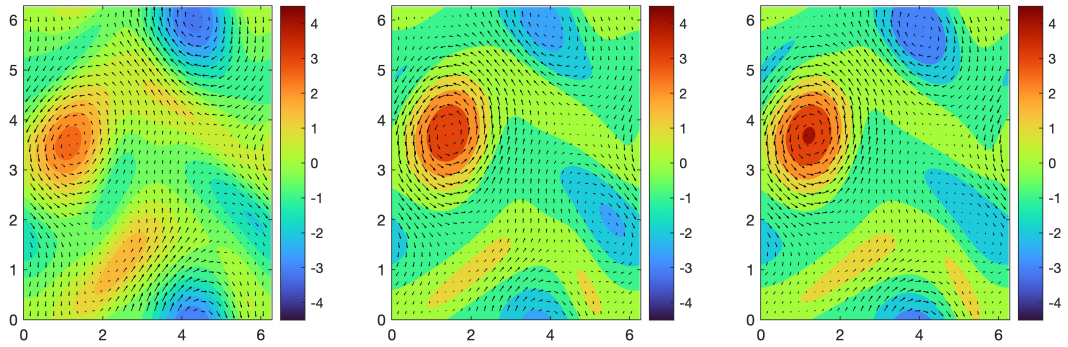
Figure 6: Evolution of the maximum magnitude of vorticity during a bursting event.

5. Conclusion

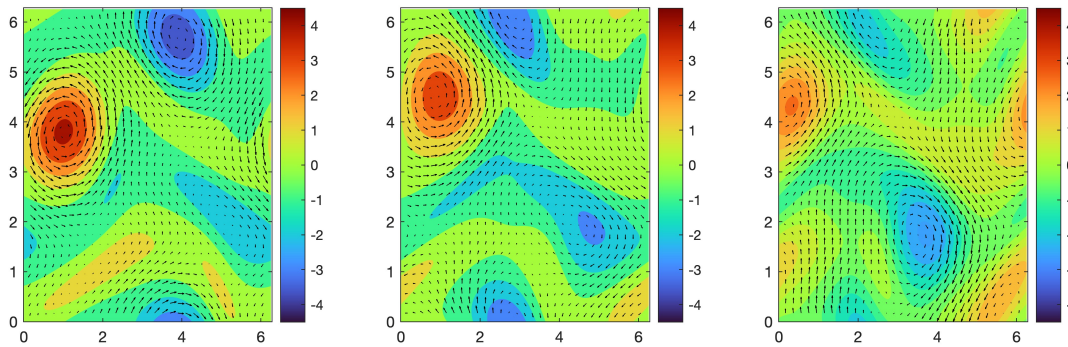
A novel second-order accurate, Forced Scalar Auxiliary Variable approach (FSAV) is introduced to preserve the underlying dissipative structure of the forced Navier-Stokes system that yields a uniform-in-time estimate of the numerical solution. As an example we apply the new algorithm to the two-dimensional incompressible Navier-Stokes equations. In the case with no-penetration and free-slip boundary condition on a simply connected domain, we are also able to derive a uniform-in-time estimate of the vorticity in H^1 norm in addition to the L^2 norm guaranteed by the general framework. Numerical results demonstrate superior performance of the new algorithm in terms of accuracy, efficiency, stability and robustness. The FSAV method is applicable to a general class of forced dissipative systems with conservative nonlinear term. In addition, the numerical scheme is autonomous if the underlying model is, laying the foundation for studying long-time dynamics of the numerical solution via dynamical system approach.

Acknowledgement

The work of D. Han is supported by the National Science Foundation grant DMS-2310340. The work of X. Wang is supported by the National Natural Science Foundation of China grant 12271237 as well as the Gary Havener Endowment. The authors share joint first authorship.



(a) snapshots at $t = 1220, 1236, 1250$.



(b) snapshots at $t = 1260, 1275, 1400$.

Figure 7: The vorticity contour and velocity field during a bursting event

References

- [1] G. AKRIVIS, B. LI, AND D. LI, *Energy-decaying extrapolated RK-SAV methods for the Allen-Cahn and Cahn-Hilliard equations*, SIAM J. Sci. Comput., 41 (2019), pp. A3703–A3727.
- [2] D. ARMBRUSTER, B. NICOLAENKO, N. SMAOUI, AND P. CHOSSAT, *Symmetries and dynamics for 2-D Navier-Stokes flow*, Phys. D, 95 (1996), pp. 81–93.
- [3] J. CARTER, D. HAN, AND N. JIANG, *Second order, unconditionally stable, linear ensemble algorithms for the magnetohydrodynamics equations*, J. Sci. Comput., 94 (2023), pp. Paper No. 41, 29.
- [4] C. FOIAS, O. MANLEY, R. ROSA, AND R. TEMAM, *Navier-Stokes equations and turbulence*, vol. 83 of Encyclopedia of Mathematics and its Applications, Cambridge University Press, Cambridge, 2001.
- [5] U. FRISCH, *Turbulence*, Cambridge University Press, Cambridge, 1995. The legacy of A. N. Kolmogorov.

- [6] V. GIRAULT AND P.-A. RAVIART, *Finite element methods for Navier-Stokes equations*, vol. 5 of Springer Series in Computational Mathematics, Springer-Verlag, Berlin, 1986. Theory and algorithms.
- [7] Y. GONG, J. ZHAO, AND Q. WANG, *Arbitrarily high-order linear energy stable schemes for gradient flow models*, *J. Comput. Phys.*, 419 (2020), pp. 109610, 20.
- [8] S. GOTTLIEB, F. TONE, C. WANG, X. WANG, AND D. WIROSOETISNO, *Long time stability of a classical efficient scheme for two-dimensional Navier-Stokes equations*, *SIAM J. Numer. Anal.*, 50 (2012), pp. 126–150.
- [9] F. GUILLÉN-GONZÁLEZ AND G. TIERRA, *On linear schemes for a Cahn-Hilliard diffuse interface model*, *J. Comput. Phys.*, 234 (2013), pp. 140–171.
- [10] T. HEISTER, M. A. OLSHANSKII, AND L. G. REBHOLZ, *Unconditional long-time stability of a velocity-vorticity method for the 2D Navier-Stokes equations*, *Numer. Math.*, 135 (2017), pp. 143–167.
- [11] J. G. HEYWOOD AND R. RANNACHER, *Finite-element approximation of the nonstationary Navier-Stokes problem. IV. Error analysis for second-order time discretization*, *SIAM J. Numer. Anal.*, 27 (1990), pp. 353–384.
- [12] A. T. HILL AND E. SÜLI, *Approximation of the global attractor for the incompressible Navier-Stokes equations*, *IMA J. Numer. Anal.*, 20 (2000), pp. 633–667.
- [13] F. HUANG AND J. SHEN, *Stability and error analysis of a class of high-order IMEX schemes for Navier-Stokes equations with periodic boundary conditions*, *SIAM J. Numer. Anal.*, 59 (2021), pp. 2926–2954.
- [14] ———, *A new class of implicit-explicit BDFk SAV schemes for general dissipative systems and their error analysis*, *Comput. Methods Appl. Mech. Engrg.*, 392 (2022), pp. Paper No. 114718, 25.
- [15] N. JIANG AND H. YANG, *Stabilized scalar auxiliary variable ensemble algorithms for parameterized flow problems*, *SIAM J. Sci. Comput.*, 43 (2021), pp. A2869–A2896.
- [16] O. A. LADYZHENSKAYA, *The mathematical theory of viscous incompressible flow*, Second English edition, revised and enlarged. Translated from the Russian by Richard A. Silverman and John Chu. Mathematics and its Applications, Vol. 2, Gordon and Breach Science Publishers, New York, 1969.
- [17] X. LI AND J. SHEN, *Error analysis of the SAV-MAC scheme for the Navier-Stokes equations*, *SIAM J. Numer. Anal.*, 58 (2020), pp. 2465–2491.

- [18] X. LI, J. SHEN, AND Z. LIU, *New SAV-pressure correction methods for the Navier-Stokes equations: stability and error analysis*, Math. Comp., 91 (2021), pp. 141–167.
- [19] L. LIN, Z. YANG, AND S. DONG, *Numerical approximation of incompressible Navier-Stokes equations based on an auxiliary energy variable*, J. Comput. Phys., 388 (2019), pp. 1–22.
- [20] A. J. MAJDA AND X. WANG, *Non-linear dynamics and statistical theories for basic geophysical flows*, Cambridge University Press, Cambridge, 2006.
- [21] A. S. MONIN AND A. M. YAGLOM, *Statistical fluid mechanics: mechanics of turbulence. Vol. I*, Dover Publications, Inc., Mineola, NY, english ed., 2007. Translated from the 1965 Russian original, Edited and with a preface by John L. Lumley, Reprinted from the 1971 edition.
- [22] L. REBHOLZ AND F. TONE, *Long-time H^1 -stability of BDF2 time stepping for 2D Navier-Stokes equations*, Appl. Math. Lett., 141 (2023), pp. Paper No. 108624, 8.
- [23] J. SHEN, J. XU, AND J. YANG, *The scalar auxiliary variable (SAV) approach for gradient flows*, J. Comput. Phys., 353 (2018), pp. 407–416.
- [24] ———, *A new class of efficient and robust energy stable schemes for gradient flows*, SIAM Rev., 61 (2019), pp. 474–506.
- [25] J. C. SIMO AND F. ARMERO, *Unconditional stability and long-term behavior of transient algorithms for the incompressible Navier-Stokes and Euler equations*, Comput. Methods Appl. Mech. Engrg., 111 (1994), pp. 111–154.
- [26] R. TEMAM, *Infinite-dimensional dynamical systems in mechanics and physics*, vol. 68 of Applied Mathematical Sciences, Springer-Verlag, New York, second ed., 1997.
- [27] F. TONE, *On the long-time stability of the Crank-Nicolson scheme for the 2D Navier-Stokes equations*, Numer. Methods Partial Differential Equations, 23 (2007), pp. 1235–1248.
- [28] F. TONE AND D. WIROSOETISNO, *On the long-time stability of the implicit Euler scheme for the two-dimensional Navier-Stokes equations*, SIAM J. Numer. Anal., 44 (2006), pp. 29–40.
- [29] X. WANG, *Approximation of stationary statistical properties of dissipative dynamical systems: time discretization*, Math. Comp., 79 (2010), pp. 259–280.
- [30] ———, *An efficient second order in time scheme for approximating long time statistical properties of the two dimensional Navier-Stokes equations*, Numer. Math., 121 (2012), pp. 753–779.
- [31] X. WANG AND Y. YU, *A note on the stability of two families of two-step schemes*, arXiv 2406.18398, (2024).

- [32] K. WU, F. HUANG, AND J. SHEN, *A new class of higher-order decoupled schemes for the incompressible Navier-Stokes equations and applications to rotating dynamics*, J. Comput. Phys., 458 (2022), pp. Paper No. 111097, 16.
- [33] X. YANG, *A novel fully-decoupled, second-order and energy stable numerical scheme of the conserved Allen-Cahn type flow-coupled binary surfactant model*, Comput. Methods Appl. Mech. Engrg., 373 (2021), p. 113502.
- [34] X. YANG AND D. HAN, *Linearly first- and second-order, unconditionally energy stable schemes for the phase field crystal equation*, J. Comput. Phys., 330 (2017), pp. 1116–1134.
- [35] X. YANG AND L. JU, *Linear and unconditionally energy stable schemes for the binary fluid-surfactant phase field model*, Comput. Methods Appl. Mech. Engrg., 318 (2017), pp. 1005–1029.
- [36] X. YANG, J. ZHAO, AND Q. WANG, *Numerical approximations for the molecular beam epitaxial growth model based on the invariant energy quadratization method*, J. Comput. Phys., 333 (2017), pp. 104–127.